Journal of Applied Physics REVIEW pubs.aip.org/aip/jap

Pyroelectric crystals for generation of neutrons: A review

Cite as: J. Appl. Phys. **135**, 200701 (2024); doi: 10.1063/5.0205453
Submitted: 26 February 2024 · Accepted: 8 May 2024 ·
Published Online: 24 May 2024

Soroush Mohtashami,[1] Hossein Afarideh,[1,a)] and Khalil Moshkbar-Bakhshayesh[1,2]

AFFILIATIONS

[1]Department of Energy Engineering and Physics, Amirkabir University of Technology, Hafez Ave., Tehran, Iran
[2]Department of Energy Engineering, Sharif University of Technology, Azadi Ave., Tehran, Iran

[a)]**Author to whom correspondence should be addressed:** hafarideh@yahoo.com

ABSTRACT

Over 2300 years ago, the discovery of tourmaline led to the understanding of pyroelectric properties, which opened new doors to various applications of pyroelectric crystal, such as neutron and x-ray generation, energy harvesting, mass spectrometry, high-voltage sources, and more. In the last two decades, researchers have carried out extensive research and development to select components and materials and innovate the design and construction of the pyroelectric neutron generator (PNG). This manuscript investigates the process and history of the PNG's development. It explains the physics governing pyroelectric crystals and the method of producing neutrons in a comprehensive and straightforward manner. Although PNGs have a lower yield and shorter lifetime compared to other neutron generators, they are still significant for research purposes due to their lack of need for an external high-voltage power supply, lower cost, smaller size, and safety. The main objective of this manuscript is to bring more attention to the research and development of PNGs. In recent years, new methods have been introduced that reduce the amount of neutron flux required for various applications. This has raised hope for the progress of commercial and industrial use of PNGs in the near future. The manuscript mentions some research cases that represent the future perspective of PNG development. Furthermore, the challenges faced by PNGs can be handled more efficiently with the utilization of generative learning algorithms and improvements in the components/mechanisms used for PNG design.

I. INTRODUCTION

In recent years, compact neutron generators (CNGs) have gained significant importance in various scientific, security, and industrial fields.[1] Some of the most important applications of the CNGs include wireless data transmission,[2] calibration of neutrino detectors in research related to neutrino and dark matter detection,[3] inspection systems for drug and explosive detection,[4] fissile material detection,[5] portable material analysis,[6,7] mine detection and ammunition separation,[8–10] industrial radiography with small dimensions,[11] geology,[12] geophysics,[13] archeology,[14] medical and biological applications,[15,16] well-logging,[17,18] neutron scattering,[19] neutron imaging,[20] activation analysis,[21] and even exploring to discover water on the planet Mars.[22] Moreover, they may be an alternative to traditional research reactors.[23]

Although, radioisotope sources have several advantages such as low production cost and the ability to achieve the appropriate particle production rate for any application, their use is limited by some obstacles. The most significant limitation is the need for the heavy and bulky shields that must be continuously present.[1] Moreover, these sources are hazardous and cannot be turned off. On the other hand, the CNGs are not subject to limitations of radioisotope sources due to their high flexibility in design and the possibility of being turned off.

The need for CNGs with different neutron production rates has led to extensive research studies and development in their design and manufacturing. Almost all of the existing and developing CNGs use deuterium–deuterium (D-D) and deuterium–tritium (D-T) fusion reactions to produce neutrons. Several types of CNGs have been designed and introduced so far, including NEUTRISTOR[24] and CNGs with field ionization ion sources.[25–27] The introduction of new CNGs that are more efficient, have a longer life span, smaller size, lower power consumption, and lower total cost makes them more applicable and could lead to further development in various fields.

Pyroelectric neutron generators (PNGs)[28] are a type of the CNG. About twenty-three centuries ago, Theophrastus, a Greek philosopher, observed that certain materials such as wood, straw, copper, and iron were absorbed by the mineral tourmaline.[29] Today, it is known that this absorption property is caused by the pyroelectric property of some types of crystals.[30] Pyroelectric crystals are anisotropic dielectric materials that are spontaneously polarized in equilibrium conditions, without any external electric field. This polarization can be changed by varying the temperature of the crystal. The change in the dipole moment of these crystals for the temperature variation of about 50 °C can create an electric field that is strong enough to produce/accelerate charged particles (i.e., electrons and ions).[31] When these charged particles collide with the appropriate targets, they can generate secondary particles such as x rays and neutrons for different applications.[32,33] Pyroelectric crystals are, also, applied for electrical energy harvesting from heat,[34] micro-analyzer probes,[35,36] mass spectrometry,[37] driver of dielectric laser accelerators,[38] pulsed gamma source,[39] pulsed neutron detection,[40] ion pump,[41] accelerator beam deflector,[42] high-voltage sources,[43] and so forth.

Almost all neutron generators require high-voltage power supplies in order to create the potential required for the fusion reaction. However, the PNG is the only reliable generator that can produce neutrons without the need for an external high-voltage power source.[28] In the PNG, the electric field required to increase the energy is provided by heating or cooling the crystal, which changes the temperature from the laboratory temperature to more than 70 °C in a vacuum environment.[44]

Compared to other CNGs, PNGs have a lower manufacturing cost and can be designed in smaller dimensions. However, the main disadvantages of the PNGs are their low yield and low lifetime.

Although the PNGs have lower yield and shorter lifetime compared to other neutron generators, study on these generators is important due to their lower cost, smaller size, and enhanced safety. Moreover, the development of new techniques that can reduce the need for a relatively high neutron flux is making PNG applications more valuable. The main objective of this manuscript is to draw more attention to the PNG research.

In this manuscript, in Sec. II, the development history of the PNG as a special kind of CNG is discussed. In Sec. III, the physics governing the pyroelectric crystal is explained and the method of producing neutrons by pyroelectric crystals is given. In Sec. IV, the future perspective of the PNG development and utilization is conferred. Section V gives the conclusion.

II. THE DEVELOPMENT HISTORY OF THE PYROELECTRIC NEUTRON GENERATOR AS A SPECIAL KIND OF COMPACT NEUTRON GENERATORS

A. Compact neutron generators

Table I lists various technologies used for neutron generation, including PNGs as a subclass of CNGs.[1,24,45–49] As mentioned, it is obvious that PNGs have a lower yield for neutron generation compared to other CNGs. However, PNGs have the advantage of not requiring a high-voltage power supply and being a cost-effective option in comparison to other techniques.

CNGs, typically involve three main processes, which include (1) ion production, usually deuterium, (2) ion acceleration, and (3) collision with a target for neutron production, usually contain

TABLE I. List of different technologies for neutron generation.

Technology		Reaction	Most common neutron yield	Most common applications
Nuclear research reactors		Fission	10^8–10^{15} n/cm^2/s	Radioisotope production, medical, imaging, materials and physics research
Nuclear fusion systems		Fusion	…	Energy
Very high energy ion accelerators (> 500 MeV)		Spallation	10^{12}–10^{15} n/cm^2/s	Materials and biology research
High energy electron accelerators (>10 MeV)		Photoneutron	10^{11}–10^{14} n/s	Radioisotope production, nondestruction testing, radiography
Medium energy ion accelerators (> 2 MeV)		Fusion	10^{12}–10^{15} n/s	Therapy, benchmark experiments, research and training
Low energy ion accelerators (CNGs) (< 400 keV)	Sealed tubes	Fusion	10^6–10^{11} n/s	Well logging, activation analysis, instruments calibration, reactor startup, moisture gauge, research and training
	Neutristor		~10^9 n/s	
	Field ionization sources		10^6–10^8 n/s	
	Plasma Focus		10^6–10^8 n/pulse	
	PNGs		10^3–10^5 n/s	
Radioisotope sources		Spontaneous fission, alpha, and gamma neutron sources	10^6–10^9 n/s	Reactor startup, mineral resources exploration, calibration, and training

deuterium or tritium atoms.[50,51] The most important part of a neutron generator is its accelerator which is usually utilized in a pulsed mode and can operate at different output levels.[52,53] Commonly, several electrodes with a cylindrical symmetry are used to form the ion accelerator with power supplies between 100 and 500 kV.[54] These electrodes focus ions to a small point of target, similar to the function of an einzel lens.[55] One of the most well-known CNGs is NEUTRISTOR which generates neutrons using a deuterium–deuterium fusion reaction. This generator is 1000 times smaller than its competitors.[56] The small size of NEUTRISTOR makes it more suitable for use in medical applications. For example, by implanting this neutron generator near a cancer tumor, the patient does not need to visit the doctor frequently, by receiving a low dose over an extended period.[57] The main challenge of NEUTRISTOR faces is the need for the high-voltage power supply. The other important types of CNGs are: penning ion source based D-D and D-T neutron generators,[58–60] electron accelerator-driven neutron source,[61] electron cyclotron resonance ion source based neutron generators,[62] and field ionization/desorption/evaporation ion source based neutron generators.[63–65]

The main difference between the PNGs and other types of CNGs is that the electric field needed to increase the ion's energy is generated by changing the crystal temperature instead of an external high-voltage power source. This feature of PNGs makes it possible to generate neutrons with the help of a low-power battery (e.g., 20 W). It should be note that since the crystal is susceptible to fast temperature changes, the rate of temperature change should not exceed 2 °C/s.[66] Therefore, the crystals need time in order of minute to produce high voltages for different applications.

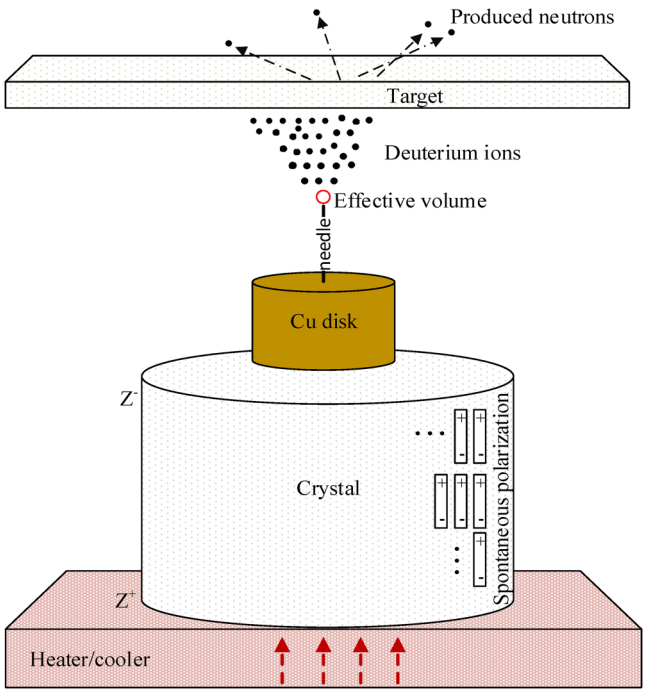

FIG. 1. The schematic view of a typical pyroelectric neutron generator.

The schematic view of a typical PNG is presented in Fig. 1. As mentioned previously, a potential of about 100 kV can be produced on the crystal's surface by heating/cooling it. By using a nano-tip needle on the crystal, the electric field can be locally enhanced and increase the deuterium ion production. The produced ions are then accelerated in the crystal's field and produce neutrons by hitting a deuterated/tritiated target.

In the following, the history and physics of neutron production by the pyroelectric crystal are reviewed and presented in detail.

B. Development history of the pyroelectric neutron generator

In 1992, Brownridge first reported the generation of x rays from a pyroelectric crystal.[67] Then, in 2001, Brownridge and Shafroth for the first time presented the results of pyroelectric accelerator tests with the ability to accelerate the electron beam to an energy of more than 100 keV.[68] They succeeded in increasing the potential of a pyroelectric electron accelerator up to 160 keV.[69] In these years, extensive research on electron/ion pyroelectric accelerators has been carried out in various universities/institutions.[70–72] In 2005, for the first time, neutron production with the help of a pyroelectric crystal and without the need for high-voltage power sources was reported. This research was conducted by Naranjo *et al.*[28] In this experiment, a tungsten needle with a tip of 100 nm and a height of 2.3 mm was placed vertically on a pyroelectric crystal made of LiTaO3 with a diameter and height of 2.5 and 0.5 cm, respectively, and the chamber containing the crystal was filled with deuterium gas with a pressure of 3.4 mTorr. The efficiency of neutron detection in the experiments was estimated to be around 18%, and the rate of neutron production in the said experiment reached about 800 neutrons/s. One year later, in 2006, under a research by Geuther and his colleagues,[73] a neutron production experiment was conducted with the help of two pyroelectric crystals with a diameter of 2 cm and a thickness of 1 cm. In these experiments, by placing two crystals facing each other, and heating/cooling them simultaneously, the potential of the accelerator increased up to two times. However, the neutron production in these experiments did not increase. In 2007, an article investigating the reasons for the low production of neutrons in this experiment was given.[74] The optimal diameter of the needle introduced needles with a tip of 70 nm for optimal neutron production experiments, while theoretically the optimal diameter of the needle was calculated to be 400 nm. In this article, the electric field required for the ionization of deuterium atoms was calculated as

$$\frac{15.4\ \text{V}}{10^{-10}\ \text{m}} = 1.54 \times 10^{11}\ \text{V/m}$$

(the ionization potential of deuterium by the size of the deuterium atom). In 2007, by changing the thermal cycle of the crystal, the number of produced deuterium ions in the accelerator was doubled, and as a result, about 2×10^5 neutrons were produced.[66] In 2008, without the use of a needle, neutrons were produced.[75] In 2009, the maximum rate of neutron production instantly reached

10^{10} neutrons per second by placing an independent ion generator and using a crystal as an accelerator of deuterium ions.[76] In 2009, a portable pyroelectric neutron generator system with suggestions to optimize the distance between two crystals, changing the deuterium gas pressure, and so forth was presented.[77] In addition, an arrangement to improve the yield of the PNG and to increase the reproducibility of the experiments was proposed.[78] In this experiment, the amounts of neutrons produced in one cycle were reported to be about 7×10^4 neutrons. In 2010, a new experimental setup to increase the potential of pyroelectric accelerator was introduced,[79] and this arrangement was used for neutron production.[80] In the same year, the PNG was introduced as one of the approved projects in the United States Defense Threat Reduction agency.[81] In 2011, for the first time, the operation of the PNG with a tritiated target was reported.[82] Nevertheless, the results of the experiments did not show much success in increasing the yield of the crystal and did not reach the initial goal of increasing the yield to more than 10^6 neutrons per thermal cycle. In 2013, the PNG with a field ionization source was used to produce ions.[83] In 2015, a report on conducting various experiments to improve the yield of the PNG was given.[84] In 2020, a new type of pyroelectric accelerator that had the ability to operate in a pulsed manner was introduced.[85] In 2022, the pyroelectric accelerator was launched with the help of infrared rays.[86]

Moreover, other studies have been conducted on pyroelectric neutron generators including a comparative study of the performance of targets containing different deuterium in the PNGs,[87] determination of the optimum needle size for the PNG,[88] investigation of abnormal changes in the current of pyroelectric accelerator in sinusoidal changes of crystal temperatures,[89] investigation of the effect of pyroelectric crystal size on the production rate of the PNG,[90,91] measurement of atom/molecule ratio of deuterium ions of the pyroelectric accelerator,[92] the production of a focused ion beam with the help of a pyroelectric accelerator,[93] the use of unconventional types of pyroelectric crystal to produce the beam (i.e., the ferroelectric ceramics),[94] the design of an indicator to know the time of occurrence of electric discharge in the crystal,[95] determining the optimal temperature change rate of the pyroelectric electron accelerator,[96] using the PNG in the calibration of neutrino and dark matter detectors,[97] and the PNGs in dynamic tests of a research reactor.[98,99]

In addition, the ferroelectric generators (FEGs) as a subclass of the pyroelectric generators can store electrically poled energy in the form of bound electric charge. This stored charge is depoled because of a phase transition occurring in the ceramic working body and charge releasing to an output circuit.[100] These generators can be high-voltage sources. As an example, an FEG with a diameter/length of 20 mm/25 mm, respectively, can generate approximately 100 kV.[101] Therefore, the FEG can be used to produce neutrons similar to the PNG. The schematic view of the significant works on the PNG is presented in Fig. 2.

III. THE PHYSICS OF NEUTRON PRODUCTION BY PYROELECTRIC CRYSTALS

A. Interaction of electrical, thermal, and mechanical characteristics of a pyroelectric crystal

In crystallography, centrosymmetry refers to the presence of an inversion center within a crystal lattice. A crystal is considered centrosymmetric if it possesses this inversion symmetry. Conversely, non-centrosymmetric crystals lack an inversion center. These non-centrosymmetric materials exhibit interesting properties due to their broken symmetry, including pyroelectricity as a subclass of piezoelectricity.[102]

Pyroelectricity is a phenomenon where certain materials generate an electric polarization in response to temperature changes. When the temperature of a pyroelectric material varies, its

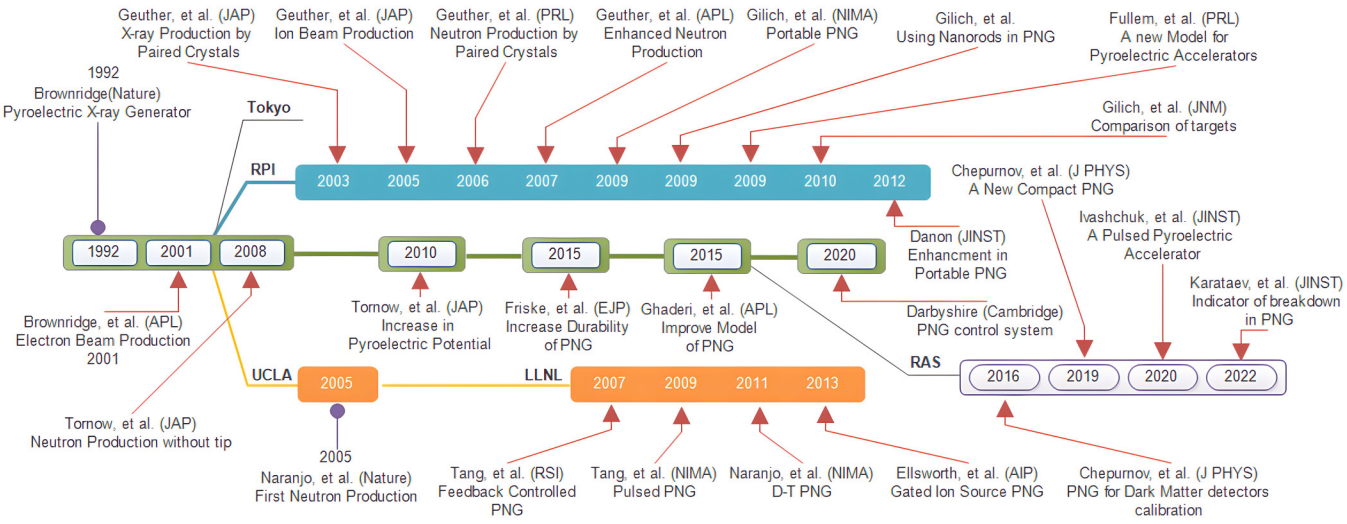

FIG. 2. The schematic view of the significant works on the PNGs.

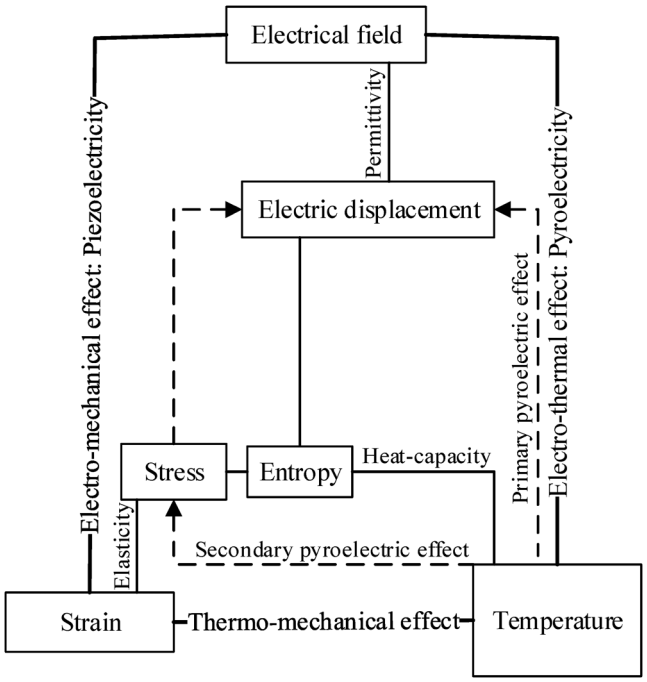

FIG. 3. Interaction among thermal, mechanical, and electrical properties for pyroelectric materials.

spontaneous polarization also changes. This effect has practical applications in various fields, including temperature sensing, energy harvesting, particle acceleration, and so forth. The pyroelectricity consists of primary and secondary effects which are discussed in the following.

Figure 3 shows the interaction of electrical, thermal, and mechanical properties in materials that exhibit pyroelectric phenomena.[102] The lines connecting each two properties (i.e., blocks) indicate that a small alteration in one property will cause a change in the others. Also, the bold lines represent the general electro-thermal, electro-mechanical, and thermo-mechanical effects.

As shown in Fig. 3, the change in temperature in the form of primary and secondary pyroelectric effects can cause a change in the electric flux density in pyroelectric materials (i.e., the dashed lines). In the primary pyroelectric effect, the temperature change has a direct effect on the electric flux density. The secondary effect, on the other hand, occurs due to the change in crystal shape, which happens as a result of the expansion or contraction of the material due to the temperature change. The change in shape creates tension in the crystal, which changes electric flux density. The relationship between primary and secondary effects of pyroelectric crystal is given by

$$\left(\frac{\partial D}{\partial T}\right)_{E,S} = \left(\frac{\partial D}{\partial T}\right)_{E,X} + \left(\frac{\partial D}{\partial x}\right)_{E,T}\left(\frac{\partial x}{\partial T}\right)_{E,S}, \quad (1)$$

where E is the electric field, D is the electric flux density (i.e., electric displacement), T is the temperature, X is the strain, and S is the stress.

The primary and secondary pyroelectric coefficients of some ferroelectric and non-ferroelectric materials are shown in Table II.[102] As can be seen, in most pyroelectric crystals, the secondary effect does not have a significant effect on the pyroelectric property of the crystal, and the primary effect is dominant. Among the mentioned crystals, two crystals, $LiTaO_3$ and $LiNbO_3$, are commonly used for the neutron production. However, reports have also been presented on the use of other crystals (e.g., SBN) as a pyroelectric generator.[103]

B. Electric charge and field generation on the surface of a pyroelectric crystal

Figure 4 shows the electric charge generation process due to the heating/cooling of a pyroelectric crystal.[102] In part (a), the pyroelectric crystal is in an equilibrium state. The spontaneous polarization in the crystal causes the absorption of free electric charges from the surrounding environment on the crystal surface, neutralizing the effect of spontaneous polarization. Part (b) shows that if two crystal surfaces are connected to an ammeter in the

TABLE II. Primary, secondary, and total pyroelectric coefficients for a number of materials at common temperatures.

Pyroelectric material	Crystal symmetry group	Total coefficient ($\mu C/m^2$ K)	Secondary pyroelectric effect	Primary pyroelectric effect
$Sr_{0.5}Ba_{0.5}Nb_2O_3$ (SBN)	4 mm	−550	−21	−529
$(NH_2CH_2COOH)_3H_2SO_4$	2	−270	+60	−330
$LiTaO_3$	3 m	−176	+2	−178
$LiNbO_3$	3 m	−83	+12/9	−95/9
$Pb_5Ge_3O_{11}$	$\bar{3}$	−95	+15/5	−110/5
$Ba_2NaNb_5O_{15}$	2 mm	−100	+41/8	−141/8
$NaNo_2$	2 mm	−140	−5	−135
$Li_2SO_4(H_2O)$	2	+86/3	+26/1	+60/2
Li_2GeO_3	2 mm	−27	−12/8	−14/2
ZnO	6 mm	−9/4	−2/5	−6/9
$BaTiO_3$	∞	−190	+80	−270

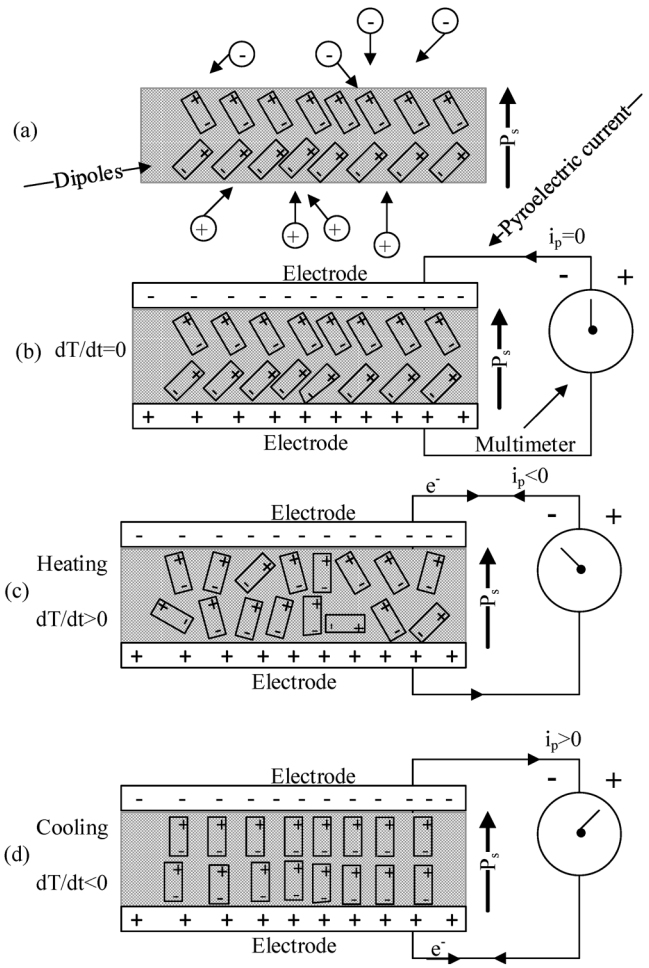

FIG. 4. A sample of pyroelectric materials including dipoles and polarization vector (a) without electrodes, (b) with electrodes connected to an ammeter at a constant temperature (c) in a heating mode, and (d) in a cooling mode.

equilibrium state, no current flows. When the pyroelectric sample is heated, the amount of polarization will be decreased, reducing the electric charge bounded to the crystal surface [see part (c)]. On the contrary, by cooling the pyroelectric crystal in part (d), the spontaneous polarization increases, reversing the direction of the produced current in the ammeter. The current produced by the pyroelectric crystal is given by

$$i_p = Ap\frac{dT}{dt}, \tag{2}$$

where i_p is the pyroelectric current, A is the crystal surface area, and p is the pyroelectric coefficient.

When an electric charge accumulates on the surface of a pyroelectric crystal due to a temperature change (e.g., 50 °C), it creates an electric field around the crystal. This electric field can be strong enough (e.g., more than 10^7 V/m) to emit electrons from the crystal surface by field emission phenomena. By hitting these produced electrons with a copper/tungsten target, x rays can be generated.[104,105] However, the electric field is not strong enough to significantly ionize the surrounding gas atoms/molecules. Therefore, in order to achieve a high ion current, the field enhancement methods are needed. The simplest method is to use needles with a very small tip diameter (i.e., between 70 and 400 nm).[74] There are some other methods for the deuterium ionization which are applied in other CNGs. Field ionization,[49,65] field emission,[106,107] field desorption and evaporation in electric field,[63,108] and microwave and radio frequency ion generation[109–111] are the main methods of ion production in the CNGs.

Figure 5 shows the schematic of an ideal model of a pyroelectric single-crystal neutron generator. It is assumed that factors such as current leakage to other parts in the gas chamber, current leakage from the surface, and nonuniformity of the charge produced by the crystal will not have a significant effect on the calculation of pyroelectric potential. In this model, considering two parallel capacitors, the electrostatic potential of the crystal can be calculated according to the amount of electric charge on the surface of the crystal (i.e., Q_{cry}) which is given by

$$\varphi = \frac{Q_{cry}}{C_{eq}} = \frac{p\,\Delta T}{\frac{\varepsilon_0\,\varepsilon_{cry}}{L_{cry}} + \frac{\varepsilon_0\,\varepsilon_{gap}}{L_{gap}}}, \tag{3}$$

where ρ is the pyroelectric coefficient, ΔT is the temperature change, C_{eq} is the capacitor equivalent value, ε_{cry} is the relative electric permeability coefficient of the crystal,[102] L_{cry} is the thickness of the crystal, and L_{gap} is the distance of the crystal to the target.

Figures 6 and 7 show the results of the calculated electric potential and electric field around the crystal by the ideal model. The potential value on the surface of a $LiTaO_3$ crystal with a pyroelectric coefficient of 176 μC/m^2 K (i.e., p), diameter of 30 mm, thickness of 1 cm, and vacuum thickness of 1.5 cm is equal to

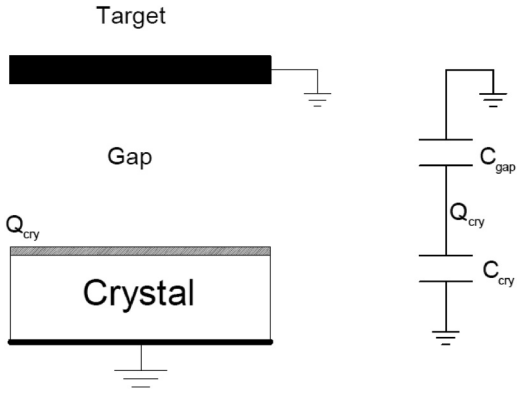

FIG. 5. Schematic of the ideal model of a pyroelectric single-crystal neutron generator.

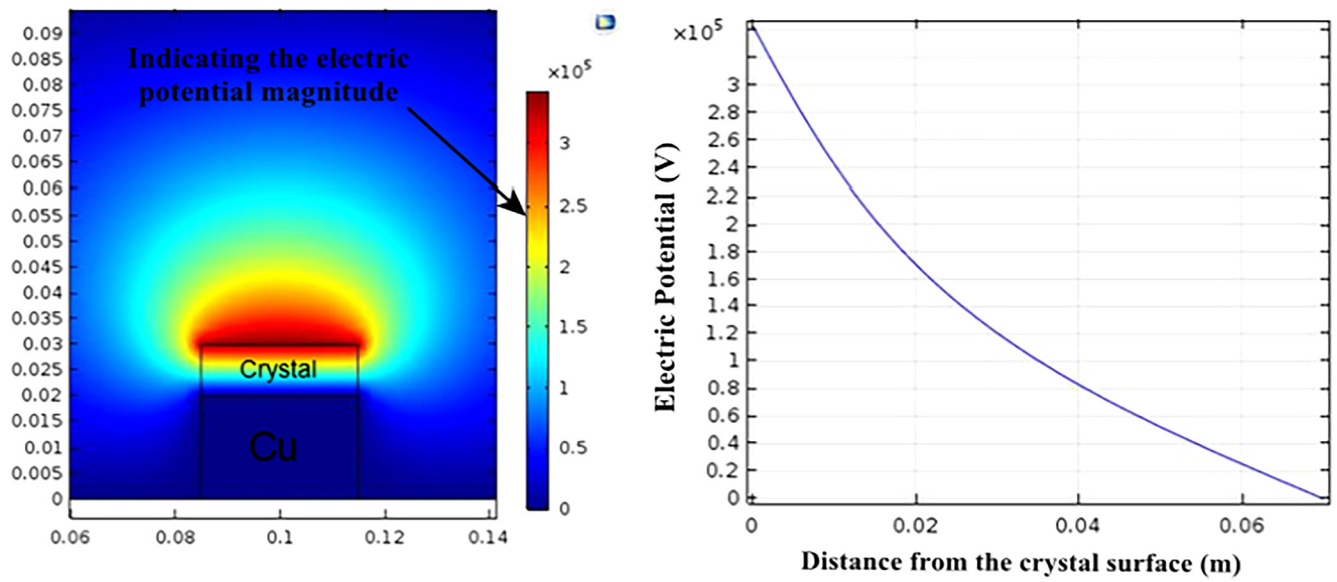

FIG. 6. The electric potential obtained around a typical pyroelectric crystal for a temperature difference of 100 °C.

about 430 kV, for 100 °C increase in temperature. However, experiments have shown that the potential value is actually about 130 kV and at its maximum reaches to 190 kV.[31] The main reason for this difference is that the ideal model does not consider the electric charge leakage from the crystal surface, which can happen through the crystal or through the space between the crystal and the target.[104] The ideal model also assumes that the crystal and vacuum have infinite resistance, which is not accurate. The amount of vacuum resistance in order to estimate the electric charge leakage cannot be easily obtained.[112] Therefore, an improved model

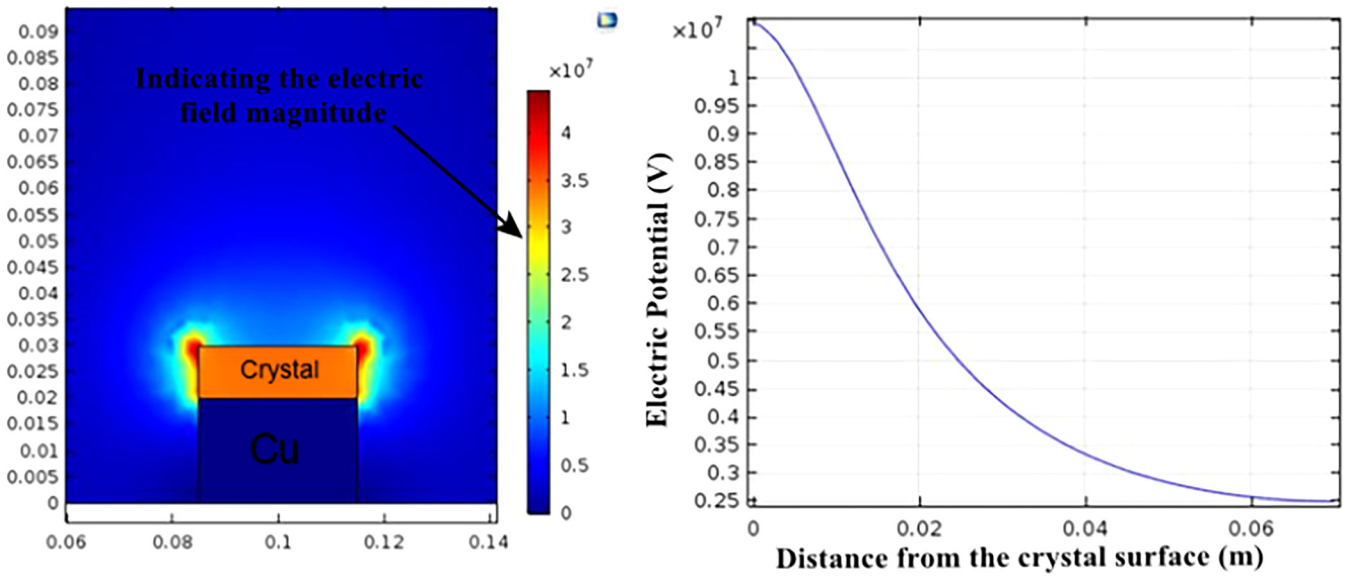

FIG. 7. The electric field obtained around a typical pyroelectric crystal for a temperature difference of 100 °C.

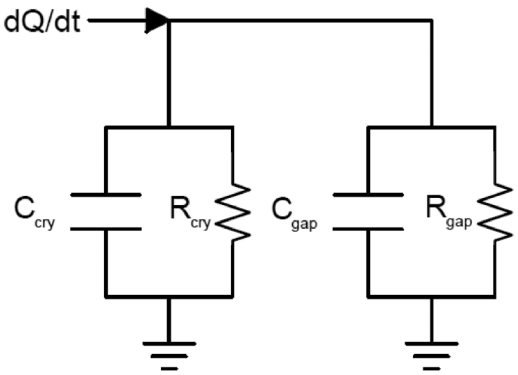

FIG. 8. The improved model of a pyroelectric accelerator.

(i.e., the most accurate model) is given by Eq. (4) which replaces the crystal potential with time variation of the potential,

$$\frac{d\varphi}{dt} = \frac{1}{C_{eq}}\frac{dQ_{cry}}{dt} = \frac{pA}{C_{eq}}\frac{dT}{dt} - \frac{\varphi}{C_{eq}R_{cry}} - \frac{\varphi}{C_{eq}R_{gap}}, \tag{4}$$

where R_{gap} and R_{cry} are resistances of vacuum and crystals, respectively, C_{eq} is the capacitor equivalent value, Q_{cry} is the crystal's surface charge, T is the crystal's temperature, φ is the crystal's potential, ρ is the pyroelectric coefficient, and A is the crystal's surface. This improved model (Fig. 8) provides a potential value that is closer to the experimental results.[104]

Using the above model and simulating the D–D and D–T interactions, theoretical maximum neutron yield/current of a typical PNG is calculated, with values of 6×10^6 and 10 nA, respectively.[113]

C. Commonly used fusion reactions and resulting neutron energy distribution

The PNG is similar to other compact and portable neutron generators that uses the D–D and D–T fusion reactions which are given by Eq. (5) produce nearly single-energy.

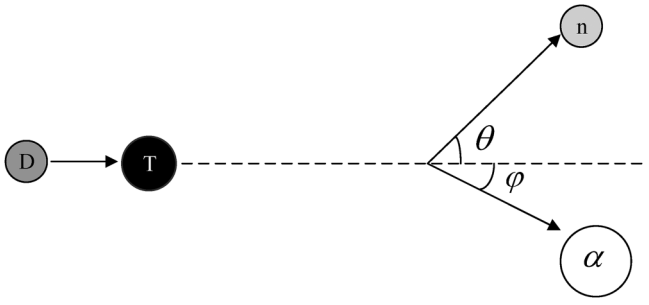

FIG. 9. D-T reaction in a laboratory system.

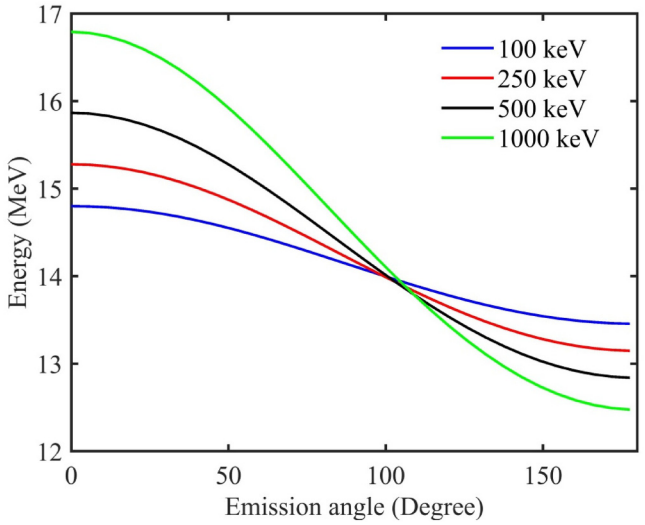

FIG. 10. The energy of the neutrons produced from the D-T interaction for different energies of the incident deuteron particle.

Considering that the Coulomb barrier between two nuclei is more than 400 keV, their interaction with low energy (e.g., 100 keV) is usually possible through the tunneling phenomenon,[114]

$$\begin{aligned} D_1^2 + D_1^2 &\rightarrow T_1^3 + H_1^1 + 4.03\ \text{MeV}, \\ D_1^2 + D_1^2 &\rightarrow He_2^3 + n_0^1 + 3.266\ \text{MeV}, \\ D_1^2 + T_1^3 &\rightarrow He_2^4 + n_0^1 + 17.588\ \text{MeV}. \end{aligned} \tag{5}$$

Targets containing deuterium/tritium are generally divided into two general categories: metal targets and organic targets. The most commonly used metal targets are titanium (TiD2), zirconium (ZrD2) and yttrium (ErD2), and the most commonly used organic targets are polyethylene (CD2) and polystyrene (CD).

In the D–T reaction, the deuterium nucleus interacts with tritium, and the resulting neutron and alpha particles scatter at φ and θ angles, respectively. This phenomenon is shown in Fig. 9. The released energy of D–T interaction is given by

$$Q = T_n\left(1 + \frac{m_n}{m_a}\right) - T_d\left(1 + \frac{m_d}{m_a}\right) - \frac{2}{m_a}\sqrt{m_d m_n T_d T_n}\cos\theta, \tag{6}$$

where T and m indicate kinetic energy and mass, respectively, and Q is the released energy. In Fig. 10, neutron energy is given according to their scattering angle for D–T interaction. As the deuterium energy increases, the energy spectrum of produced neutrons becomes wider. Additionally, neutrons scattered in the direction of deuterium momentum have the highest energy, while the opposite direction has the lowest energy.[115]

IV. THE FUTURE PERSPECTIVE OF THE PNG DEVELOPMENT AND UTILIZATION

No need for a high-voltage power supply, safer, and small size are some characteristics of the PNGs making them a potentially

suitable type of neutron generator for various applications. However, they also have some challenges such as lower yield and shorter lifetime, which need to be addressed for practical applications of PNGs.

There are two ways to achieve this goal. First, we can increase the yield of the PNG by using optimization methods and generative learning algorithms[116] in the design and construction of the PNG. Second, we can improve and optimize the performance and efficiency of analyzing techniques utilizing neutrons such as PGNAA, NAA, neutron imaging, etc.[117,118] by using soft computing techniques such as fuzzy systems, neural networks, and evolutionary algorithms.

For instance, optimization of the PNG to achieve the maximum possible neutron yield,[119] optimization of thermalization devices using multi-layer perceptron neural network for maximizing/minimizing thermal flux/non-thermal flux,[120] PGNAA optimization based on signal-to-noise ratio evaluation,[121] NAA device optimization,[122] reduction the number of projection/time usage for neutron tomography using artificial neural networks,[123] utilization of deep convolutional neural networks for obtaining high-quality reconstructions from sparse-view and low signal-to-noise ratio,[124] resolution enhancement of neutron radiography image using convolutional neural networks,[125] and so forth may be applied to improve the yield and utilization of PNGs.

Moreover, investigating the use of iridium needle instead of tungsten in the pyroelectric generator effect on increasing the lifespan and efficiency of the generator, applying other heating methods, such as using infrared lasers for heating the crystal and examining its effect on the generator's radiation dynamics, determining the optimal profile of the temperature change of the crystal in order to increase the yield of the pyroelectric generator, surveying the effect of different temperature ranges of the crystal (e.g., 0–50 °C instead of 20–70 °C) on the neutron yield of the crystal, optimizing the dimensions of the plate under crystal to prevent electrical failure in the pyroelectric generator, investigating the possibility of using other types of pyroelectric crystals such as SBN, and utilizing various types of resistors capable of withstanding high voltage between the needle and the crystal may be appropriate for increasing the PNGs yield.[126] Finally, some recent research in halide perovskite and molecular crystals has discovered new non-centrosymmetric crystals with giant pyroelectricity. Utilizing them in the PNGs can significantly improve their neutron yield and durability.[127]

V. CONCLUSION

Pyroelectric crystals have already shown their ability in many applications including neutron and x-ray generation, radiation detection, energy harvesting, micro-analyzer probes, high-voltage sources, and so forth. For utilization of pyroelectric crystal as a neutron generator, nearly two decades of research and development have been carried out in the selection of components/materials and innovations for the PNG design. The PNG does not need any high-voltage power sources to produce neutrons. This makes this type of generator potentially the most interesting and the smallest neutron generator available. Despite this significant advantage, it is necessary to increase the neutron production yield and lifetime of the PNGs in order to use them efficiently in industrial and security applications. With the growing use of artificial intelligence methods in optimizing neutron analyzing systems, the required neutron flux for various applications is expected to decrease over time. The hope is that in the near future, commercial and industrial use of portable neutron generators in different fields will advance, similar to pyroelectric x-ray generators. Additionally, by utilizing generative learning algorithms and improving the components and mechanisms used in portable neutron generator designs, it may be possible to more effectively address the challenges associated with these generators.

AUTHOR DECLARATIONS

Conflict of Interest

The authors have no conflicts to disclose.

Author Contributions

Soroush Mohtashami: Conceptualization (equal); Investigation (equal); Methodology (equal); Project administration (equal); Resources (equal); Supervision (equal); Writing – review & editing (equal). **Hossein Afarideh:** Resources (equal); Supervision (equal); Writing – review & editing (equal). **Khalil Moshkbar-Bakhshayesh:** Conceptualization (equal); Investigation (equal); Methodology (equal); Resources (equal); Visualization (equal); Writing – original draft (equal).

DATA AVAILABILITY

The data that support the findings of this study are available from the corresponding author upon reasonable request.

REFERENCES

[1]I. Radia and Y. Rep, IAEA radiation technology reports series, ISSN, 2225 (IAEA, 2012).
[2]M. J. Joyce, M. D. Aspinall, M. Clark, E. Dale, H. Nye, A. Parker, L. Snoj, and J. Spires, Nucl. Instrum. Methods Phys. Res., Sect. A **1021**, 165946 (2022).
[3]A. Chepurnov, M. Gromov, V. Y. Ionidi, A. Kaplii, M. Kirsanov, A. Klenin, D. Kolesnikov, A. Kubankin, A. Y. Maslenkina, and A. Oleinik, *Compact Neutron Generators for the Calibration of low Background Experiments* (IOP Publishing, 2019), p. 012103.
[4]C. Moss, M. Brener, C. Hollas, and W. Myers, Nucl. Instrum. Methods Phys. Res., Sect. B **241**, 793 (2005).
[5]P. Hausladen, P. Bingham, J. Neal, J. Mullens, and J. Mihalczo, Nucl. Instrum. Methods Phys. Res., Sect. B **261**, 387 (2007).
[6]S.-W. Jing, D.-S. Gu, S. Qiao, Y.-R. Liu, L.-M. Liu, and J. Shi-Wei, Rev. Sci. Instrum. **76**, 045110 (2005).
[7]S.-Y. Chen, G.-H. Li, S.-L. Jia, Z.-H. Lu, D.-D. He, G. Ke, G.-Y. Shi, and S.-W. Jing, in *Design and Optimization of a PGNAA System Based on DD Neutron Generator for Cement Composition Analysis* (American Society of Mechanical Engineers, 2022), p. V015T16A067.
[8]H. Xue, D.-D. He, K. Gong, S.-W. Jing, and Y.-L. Zheng, Nucl. Instrum. Methods Phys. Res., Sect. B **482**, 82 (2020).
[9]G. Viesti, M. Lunardon, G. Nebbia, M. Barbui, M. Cinausero, G. D'Erasmo, M. Palomba, A. Pantaleo, J. Obhođaš, and V. Valković, Appl. Radiat. Isot. **64**, 706 (2006).
[10]D. Sudac, S. Majetic, R. Kollar, K. Nad, J. Obhodas, and V. Valkovic, IEEE Trans. Nucl. Sci. **59**, 1421 (2012).

[11]M. Taylor, E. Sengbusch, C. Seyfert, E. Moll, and R. Radel, Phys. Procedia **88**, 175 (2017).
[12]M. Ayllon, P. A. Adams, J. C. Batchelder, J. D. Bauer, T. A. Becker, L. A. Bernstein, S.-A. Chong, J. James, L. E. Kirsch, and K.-N. Leung, Nucl. Instrum. Methods Phys. Res., Sect. A **903**, 193 (2018).
[13]M. Borsaru, in *Selected Topics in Nuclear Geophysics* (Citeseer, 2005), p. 2005.
[14]A. Miceli, G. Festa, G. Gorini, R. Senesi, and C. Andreani, Meas. Sci. Technol. **24**, 125903 (2013).
[15]S. Jing, H. Guo, Y. Qi, G. Yang, and Y. Huang, Appl. Radiat. Isot. **160**, 109138 (2020).
[16]N. Marchese, A. Cannuli, M. Caccamo, and C. Pace, Biochim. Biophys. Acta **1861**, 3661 (2017).
[17]A. X. Chen, A. J. Antolak, and K.-N. Leung, Nucl. Instrum. Methods Phys. Res., Sect. A **684**, 52 (2012).
[18]T. Anniyev, M. Vasilyev, V. Khabashesku, and F. Inanc, IEEE Trans. Nucl. Sci. **67**, 1885 (2020).
[19]J. Csikai, At. Energy Rev. **11**, 415 (1973).
[20]J. Brenizer, Phys. Procedia **43**, 10 (2013).
[21]Y. Kiyanagi, AAPPS Bull. **31**, 1 (2021).
[22]D. Lisov, M. Litvak, A. Kozyrev, I. Mitrofanov, and A. Sanin, Astron. Lett. **44**, 482 (2018).
[23]D. Banks and Z. Tun, Technical report-652, Sylvia Fedoruk Canadian Centre for Nuclear Innovation 653 (2019).
[24]J. M. Elizondo-Decanini, D. Schmale, M. Cich, M. Martinez, K. Youngman, M. Senkow, S. Kiff, J. Steele, R. Goeke, and B. Wroblewski, IEEE Trans. Plasma Sci. **40**, 2145 (2012).
[25]A. Chepurnov, V. Ionidi, O. Ivashchuk, M. Kirsanov, E. Kitsyuk, A. Klenin, A. Kubankin, R. Nazhmudinov, I. Nikulin, and A. Oleinik, J. Instrum. **13**, C02035 (2018).
[26]K.-N. Leung, Nucl. Technol. **206**, 1607 (2020).
[27]A. Persaud, O. Waldmann, R. Kapadia, K. Takei, A. Javey, and T. Schenkel, Rev. Sci. Instrum. **83**, 02B312 (2012).
[28]B. Naranjo, J. K. Gimzewski, and S. Putterman, Nature **434**, 1115 (2005).
[29]F. C. Hawthorne and D. J. Henry, "Classification of the minerals of the tourmaline group," Eur. J. Mineral. **11**, 201 (1999).
[30]F. C. Hawthorne and D. J. Henry, "Classification of the minerals of the tourmaline group," Eur. J. Mineral. **11**, 201 (1999).
[31]S. Mohtashami, H. Afarideh, F. A. Davani, and R. Ghaderi, J. Instrum. **16**, P10017 (2021).
[32]D. J. Gillich, *Particle Acceleration with Pyroelectric Crystals* (Rensselaer Polytechnic Institute, 2009).
[33]Y. Danon, *A Novel Compact Pyroelectric X-Ray and Neutron Source* (Rensselaer Polytechnic Inst., Troy, NY (United States), 2007).
[34]C. R. Bowen, J. Taylor, E. LeBoulbar, D. Zabek, A. Chauhan, and R. Vaish, Energy Environ. Sci. **7**, 3836 (2014).
[35]S. Imashuku, A. Imanishi, and J. Kawai, Rev. Sci. Instrum. **84**, 073111 (2013).
[36]S. Imashuku and K. Wagatsuma, Rev. Sci. Instrum. **88**, 023117 (2017).
[37]E. L. Neidholdt and J. Beauchamp, Anal. Chem. **79**, 3945 (2007).
[38]R. Yoder, Z. Kabilova, and B. Saeks, Proc. IPAC **16**, 1604 (2016).
[39]A. Chen, A. Antolak, K.-N. Leung, T. Raber, and D. Morse, in *Pulsed Pyroelectric Crystal-Powered Gamma Source* (American Institute of Physics, 2013), p. 720.
[40]W. Liang, Y. Lu, J. Wu, H. Gao, and M. Li, Nucl. Instrum. Methods Phys. Res., Sect. A **827**, 161 (2016).
[41]K. Vinayakumar, V. Gund, and A. Lal, J. Vac. Sci. Technol. B **39**, 024202 (2021).
[42]A. Oleinik, A. Kubankin, R. Nazhmudinov, K. Vokhmyanina, A. Shchagin, and P. Karataev, J. Instrum. **11**, P08007 (2016).
[43]D. Ni, V. Gund, and A. Lal, in *PCB Integrated Linbo3 Pyroelectric High Voltage Supply with Electrostatic Switch Regulator* (IEEE, 2021), p. 968.
[44]J. A. Geuther and Y. Danon, Nucl. Instrum. Methods Phys. Res., Sect. B **261**, 110 (2007).
[45]A. K. Gillespie, C. Lin, and R. Duncan, Nucl. Eng. Technol. (in press).
[46]A. Cannuli, M. T. Caccamo, N. Marchese, E. A. Tomarchio, C. Pace, and S. Magazù, "Indoor Fast Neutron Generator for Biophysical and Electronic Applications," J. Phys. conf. Ser. **1014**, 012001 (2018).
[47]R. Niranjan, R. Srivastava, J. Joycee, and K. Joshi, Plasma Phys. Controlled Fusion **65**, 075010 (2023).
[48]I. S. Anderson, C. Andreani, J. M. Carpenter, G. Festa, G. Gorini, C. K. Loong, and R. Senesi, "Research opportunities with compact accelerator-driven neutron sources," Phys. Rep. **654**, 1 (2016).
[49]J. Ellsworth, S. Falabella, J. Sanchez, V. Tang, and H. Wang, J. Appl. Phys. **116**, 193301 (2014).
[50]J. Reijonen, in *Compact Neutron Generators for Medical, Home Land Security, and Planetary Exploration* (IEEE, 2005), p. 49.
[51]G. J. Csikai, *CRC handbook of fast neutron generators* (CRC Press, London, UK, 1987)
[52]J. Gow and H. Pollock, Rev. Sci. Instrum. **31**, 235 (1960).
[53]R. Walko and G. Rochau, IEEE Trans. Nucl. Sci. **28**, 1531 (1981).
[54]H. L. v. d. Horst, *Gas-Discharge Tubes* (Philips Technical Library, 1964).
[55]H. Liebl, *Applied Charged Particle Optics* (Springer, 2008), Vol. 2012.
[56]J. M. Elizondo, "NEUTRISTOR 2012-R&D 100 Award report" (2012).
[57]B. Dodson, "World's smallest neutron generator – it's not just for nukes anymore," http://www.gizmag.com/sandianeutristor-neutron-generator-chip/23856/ (2013)
[58]B. K. Das, A. Shyam, R. Das, and A. Rao, Instrum. Exp. Tech. **56**, 130 (2013).
[59]T. P. Lou, *Compact DD/DT Neutron Generators and Their Applications* (University of California, Berkeley, 2003).
[60]T. Czakoj, M. Košťál, M. Zmeškal, E. Novák, F. Mravec, F. Cvachovec, J. Šimon, M. Schulc, R. Uhlář, and P. Alexa, Nucl. Instrum. Methods Phys. Res., Sect. A **1034**, 166837 (2022).
[61]I. Anderson, C. Andreani, J. Carpenter, G. Festa, G. Gorini, C.-K. Loong, and R. Senesi, Phys. Rep. **654**, 1 (2016).
[62]V. Skalyga, I. Izotov, S. Golubev, A. Sidorov, S. Razin, A. Strelkov, O. Tarvainen, H. Koivisto, and T. Kalvas, J. Appl. Phys. **118**, 093301 (2015).
[63]B. Bargsten Johnson, P. Schwoebel, P. Resnick, C. Holland, K. Hertz, and D. Chichester, J. Appl. Phys. **114**, 174906 (2013).
[64]B. Reichenbach, I. Solano, and P. Schwoebel, J. Appl. Phys. **103**, 094912 (2008).
[65]B. B. Johnson, P. Schwoebel, C. Holland, P. Resnick, K. Hertz, and D. Chichester, Nucl. Instrum. Methods Phys. Res., Sect. A **663**, 64 (2012).
[66]V. Tang, G. Meyer, J. Morse, G. Schmid, C. Spadaccini, P. Kerr, B. Rusnak, S. Sampayan, B. Naranjo, and S. Putterman, Rev. Sci. Instrum. **78**, 123504 (2007).
[67]J. D. Brownridge, Nature **358**, 287 (1992).
[68]J. Brownridge, S. Shafroth, D. Trott, B. Stoner, and W. Hooke, Appl. Phys. Lett. **78**, 1158 (2001).
[69]J. D. Brownridge and S. M. Shafroth, Appl. Phys. Lett. **83**, 1477 (2003).
[70]J. A. Geuther and Y. Danon, J. Appl. Phys. **97**, 074109 (2005).
[71]J. Geuther, Y. Danon, F. Saglime, and B. Sones, in *Electron Acceleration for X-Ray Production Using Paired Pyroelectric Crystals* (Rensselaer Polytechnic Inst., Troy, NY (United States), 2003), p. 124.
[72]N. Kukhtarev, J. Kukhtareva, M. Bayssie, J. Wang, and J. Brownridge, J. Appl. Phys. **96**, 6794 (2004).
[73]J. Geuther, Y. Danon, and F. Saglime, Phys. Rev. Lett. **96**, 054803 (2006).
[74]J. A. Geuther and Y. Danon, Appl. Phys. Lett. **90**, 174103 (2007).
[75]W. Tornow, S. Shafroth, and J. Brownridge, J. Appl. Phys. **104**, 034905 (2008).
[76]V. Tang, G. Meyer, S. Falabella, G. Guethlein, S. Sampayan, P. Kerr, B. Rusnak, and J. Morse, J. Appl. Phys. **105**, 026103 (2009).
[77]D. Gillich, A. Kovanen, B. Herman, T. Fullem, and Y. Danon, Nucl. Instrum. Methods Phys. Res., Sect. A **602**, 306 (2009).
[78]D. J. Gillich, R. Teki, T. Z. Fullem, A. Kovanen, E. Blain, D. B. Chrisey, T.-M. Lu, and Y. Danon, Nano Today **4**, 227 (2009).
[79]W. Tornow, S. Lynam, and S. Shafroth, J. Appl. Phys. **107**, 063302 (2010).

[80]W. Tornow, W. Corse, S. Crimi, and J. Fox, Nucl. Instrum. Methods Phys. Res., Sect. A **624**, 699 (2010).
[81]T. Anderson, R. Edwards, K. Bright, A. Kovanen, Y. Danon, B. Moretti, J. Musk, M. Shannon, and D. Gillich, in *Preliminary Results From Pyroelectric Crystal Accelerator* (American Institute of Physics, 2011), p. 767.
[82]B. Naranjo, S. Putterman, and T. Venhaus, Nucl. Instrum. Methods Phys. Res., Sect. A **632**, 43 (2011).
[83]J. Ellsworth, V. Tang, S. Falabella, B. Naranjo, and S. Putterman, in *Neutron Production Using a Pyroelectric Driven Target Coupled with a Gated Field Ionization Source* (American Institute of Physics, 2013), p. 128.
[84]E. Friske, G. Deuter, and J. Jochum, Eur. Phys. J. A **51**, 1 (2015).
[85]O. Ivashchuk, A. Shchagin, A. Kubankin, V. Ionidi, A. Chepurnov, V. Miroshnik, V. Volkov, and D. Lepeshko, J. Instrum. **15**, C02002 (2020).
[86]R. Nazhmudinov, A. Kubankin, A. Oleinik, and A. Klenin, in *Observation of X-Rays During Heating a Pyroelectric Crystal by an Infrared Laser* (IOP Publishing, 2022), p. 012001.
[87]D. J. Gillich, A. Kovanen, and Y. Danon, J. Nucl. Mater. **405**, 181 (2010).
[88]D. Gillich, Y. Danon, A. Kovanen, B. Herman, and W. Labarre, Trans. Am. Nucl. Soc. **98**, 393 (2008).
[89]A. Oleinik, M. Gilts, P. Karataev, A. Klenin, and A. Kubankin, J. Appl. Phys. **132**, 204101 (2022).
[90]A. Kovanen, D. Gillich, T. Fullem, and Y. Danon, in *DD Nuclear Fusion Using Different Size Pyroelectric Crystals* (IEEE, 2009), p. 1989.
[91]M. Valikhani and M. Habibi, J. Fusion Energy **36**, 92 (2017).
[92]D. Gillich, Y. Danon, J. A. Geuther, B. Marus, and B. McDermott, Trans. Am. Nucl. Soc. **97**, 927 (2007).
[93]T. Fullem, A. Kovanen, D. Gillich, and Y. Danon, in *Focused ion Beam Production Using a Pyroelectric Crystal and a Resistive Glass Tube* (IEEE, 2009), p. 282.
[94]A. Shchagin, V. Miroshnik, V. Volkov, and A. Oleinik, Appl. Phys. Lett. **107**, 233505 (2015).
[95]P. Karataev, A. Oleinik, K. Fedorov, A. Klenin, A. Kubankin, and A. Shchagin, Appl. Phys. Express **15**, 066001 (2022).
[96]A. Kubankin, A. Chepurnov, O. Ivashchuk, V. Y. Ionidi, I. Kishin, A. Klenin, A. Oleinik, and A. Shchagin, AIP Adv. **8**, 035207 (2018).
[97]A. Chepurnov, V. Ionidi, M. Gromov, M. Kirsanov, A. Klyuyev, A. Kubankin, A. Oleinik, A. Shchagin, and K. Vokhmyanina, in *Development of Pyroelectric Neutron Source for Calibration of Neutrino and Dark Matter Detectors* (IOP Publishing, 2017), p. 012119.
[98]A. Darbyshire, Thesis (University of Cambridge, Cambridge, England, 2020.
[99]A. Darbyshire and K. Atkinson, NPIC HMIT **11**, 1972 (2017).
[100]D. W. Bolyard, A. A. Neuber, J. T. Krile, and M. Kristiansen, IEEE Trans. Plasma Sci. **38**, 1008 (2010).
[101]L. Altgilbers, in *Recent Advances in the Development of Ferroelectric Generators* (IEEE, 2013), p. 1.
[102]A. K. Batra and M. D. Aggarwal, *Pyroelectric Materials: Infrared Detectors, Particle Accelerators, and Energy Harvesters* (SPIE Press, Bellingham, USA, 2013).
[103]V. Andrianov, A. Erzinkian, L. Ivleva, and P. Lykov, AIP Adv. **7**, 115313 (2017).
[104]T. Fullem and Y. Danon, J. Appl. Phys. **106**, 074101 (2009).
[105]H. Kusano, Y. Oyama, M. Naito, H. Nagaoka, H. Kuno, E. Shibamura, N. Hasebe, Y. Amano, K. J. Kim, and J. A. M. Lopes, in *Development of an X-Ray Generator Using a Pyroelectric Crystal for X-Ray Fluorescence Analysis on Planetary Landing Missions* (SPIE, 2014), p. 199.
[106]S. Jo, Y. Tu, Z. Huang, D. Carnahan, D. Wang, and Z. Ren, Appl. Phys. Lett. **82**, 3520 (2003).
[107]Z. Xie, Z. Chen, Z. Xu, J. Zhang, and H. Li, in *Field Ion Emission Property of Carbon Nanotube Arrays* (IEEE, 2014), p. 1.
[108]K. L. Hertz, B. B. Johnson, C. E. Holland, P. J. Resnick, P. R. Schwoebel, and D. L. Chichester, in *A Microfabricated Electrostatic Field Desorption ion Source* (IEEE, 2012), p. 1434.
[109]M. Muramatsu, S. Hojo, Y. Iwata, K. Katagiri, Y. Sakamoto, N. Takahashi, N. Sasaki, K. Fukushima, K. Takahashi, and T. Suzuki, Rev. Sci. Instrum. **87**, 02C110 (2016).
[110]J. Reijonen, M. Eardley, R. Gough, K. Leung, and R. Thomae, Nucl. Instrum. Methods Phys. Res., Sect. A **511**, 301 (2003).
[111]J. Reijonen, F. Gicquel, S. Hahto, M. King, T.-P. Lou, and K.-N. Leung, Appl. Radiat. Isot. **63**, 757 (2005).
[112]K. Hanamoto, T. Kataoka, and K. Yamaoka, Appl. Radiat. Isot. **185**, 110230 (2022).
[113]S. Mohtashami, H. Afarideh, F. A. Davani, and R. Ghaderi, J. Instrum. **17**, P11015 (2022).
[114]W. E. Meyerhof and W. E. Meyerhof, *Elements of Nuclear Physics* (McGraw-Hill, New York, 1967), Vol. 174.
[115]S. Mohtashami and K. Moshkbar-Bakhshayesh, "A new approach for simulating DT fusion interaction using the Geant4 toolkit," J. Instrum. **17**, T03005 (2022).
[116]A. Ng, "Generative learning algorithms," Stanford Lecture Notes 5, part 4, (2008).
[117]L. A. Zadeh, in *Fuzzy Sets, Fuzzy Logic, and Fuzzy Systems: Selected Papers by Lotfi A. Zadeh* (World Scientific, 1996), p. 775.
[118]I. Ramezani, K. Moshkbar-Bakhshayesh, N. Vosoughi, and M. B. Ghofrani, Prog. Nucl. Energy **149**, 104253 (2022).
[119]A. M. Daskalakis, Thesis (Rensselaer Polytechnic Institute, Troy, NY, 2011).
[120]M. Zolfaghari, S. F. Masoudi, F. Rahmani, and A. Fathi, Sci. Rep. **12**, 8635 (2022).
[121]J. Li, W. Jia, D. Hei, Z. Yao, and C. Cheng, Nucl. Eng. Technol. **54**, 2221 (2022).
[122]M. Masoumi, S. F. Masoudi, and F. Rahmani, Nucl. Eng. Technol. **55**, 4246 (2023).
[123]D. Micieli, T. Minniti, L. M. Evans, and G. Gorini, Sci. Rep. **9**, 2450 (2019).
[124]S. Venkatakrishnan, A. Ziabari, J. Hinkle, A. W. Needham, J. M. Warren, and H. Z. Bilheux, Mach. Learn.: Sci. Technol. **2**, 025031 (2021).
[125]M. L. Yahiaoui, F. Kharfi, and L. Boukerdja, Nucl. Instrum. Methods Phys. Res., Sect. A **1050**, 168123 (2023).
[126]S. Mohtashami, Thesis (Amirkabir University of Technology, Tehran, Iran, 2023).
[127]S. Shahrokhi, W. Gao, Y. Wang, P. R. Anandan, M. Z. Rahaman, S. Singh, D. Wang, C. Cazorla, G. Yuan, and J. M. Liu, Small Methods **4**, 2000149 (2020).